Transactions of the Korean Nuclear Society Spring Meeting
Jeju, Korea, May 18-19, 2017

A Feasibility Study to characterize the performance at RIKEN compact neutron source

Jin Man Kim[a], Jongyul Kim[b], ChangHee Lee[a], Atsushi Taketani[c], Yasuo Wakabayashi[c], Yoshie Otake[c], Makoto Goto[c], Takao Hashiguchi[c] and TaeJoo Kim[a,*]
[a]*Neutron Science Division, Korea Atomic Energy Research Institute, DaeJeon, 34057, Korea*
[b]*Neutron Instrumentation Division, Korea Atomic Energy Research Institute, DaeJeon, 34057,Korea*
[c]*RIKEN Center for Advanced Photonics, RIKEN, 2-1 Hirosawa, Wako, Saitama, 351-0198 Japan*
[*]*Corresponding author: tj@kaeri.re.kr*

1. Introduction

Neutron imaging technique is an important tool in Non-Destructive Test (NDT), which has been widely adopted in industrial, medical, metallurgical, nuclear and explosive inspections [1]. Neutron imaging technique must need high neutron flux in order to apply more scientific applications and many nuclear reactors or high-power spallation sources, such as ISIS, J-PARC and SNS facilities have been realized [2]. However, because of costs and the mobility problem, there is a limitation to the application and development of new research fields of neutron imaging. By the way, employing low-energy (~10 to 100 MeV) proton on low-Z targets (e.g., Li, Be) permits the use of compact accelerator-driven neutron sources (CANS). The CANS, due to their modesty in scale and operation costs, and flexibility in instrumental configuration, are ideal to play a complementary role with respect to high-power neutron source. Therefore, the world community has increasingly recognized the value of CANS. Recently, aiming for industrial use, as well as for transportable neutron imaging system development, RIKEN Accelerator-driven compact Neutron Source(RANS) of 7.0 MeV proton energy has been designed and constructed successfully with the concept of long life, low cost, light weight, compact size, proper neutron flux and enough safety. In this study, we investigated the characteristics and performance of RANS using standard samples and representative results are presented.

2. Experimental Setup

2.1 Compact Neutron Source

The RANS is RIKEN Accelerator-driven compact Neutron Source 7.0 MeV proton energy and has four major parts, which are a proton linear accelerator, a target station, neutron guides, and a camera box as shown in Fig.1 [3]. Total length is 15 m and the accelerator part is 8 m. Protons are accelerated up to an energy of 7 MeV with a maximum average current of 100 A by a Model PL-7 linear accelerator. Fig.2 shows a sketch of the setup from the target station to the camera box. The protons bombard a beryllium target at the center of the target station [3, 4] and then neutrons are generated via the Be(p,n) reaction. The neutrons are slowed by hydrogens in a moderator, downstream, of the beryllium target made of 40 mm-thick polyethylene. Finally, the neutrons from the moderator surface propagate to the downstream camera box through the neutron guides. The size of beam port is 15 cm × 15 cm. The camera box and the neutron guides are shielded by borated polyethylene. There are a large number of thermal neutrons with energy around 25 meV and fast neutrons with energy around a few MeV[5,6]. The angular divergence of the thermal neutron beam at the sample position is 0.03 rad. In this study, thermal neutrons were used to take neutron images.

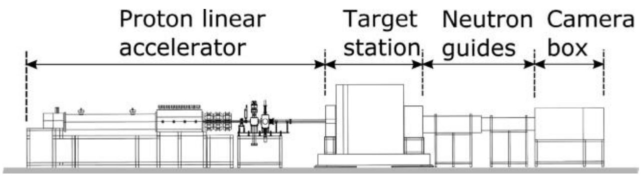

Fig. 1. Schematic diagram of the RANS [3].

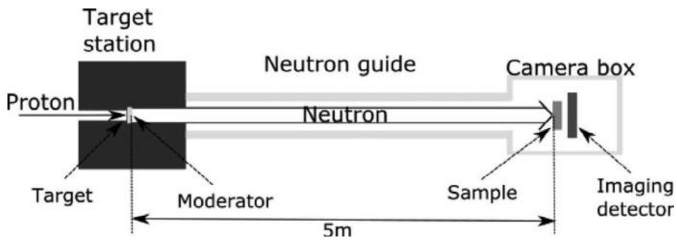

Fig. 2. Schematic diagram from the target station to the camera box[3].

2.2 Detecting System for Imaging

The imaging detecting system was set in the camera box. The thermal neutrons transmitted through the sample impact on the LiF/ZnS scintillator and generate alpha and tritium particles. Then they generate scintillation photons in the scintillator. The photons propagate to a cooled CCD sensor (BITRAN BU-53LN) through a mirror and a focusing lens. The number of photons reaching the CCD sensor is proportional to the neutron intensity at the scintillator. The image sensor is mainly sensitive to thermal neutrons, because fast neutrons make a much smaller contribution to the generation of scintillation photons. The size of the pixels on the image sensor is 80 × 80 μm^2. The size of the sensitive area is 146 mm × 106 mm, respectively [3].

2.3 Standard Samples and Test Condition

We utilized the standard specimens and procedures described in ASTM 545-05 for this experiment [7]. Two types of image quality indicators (Beam Purity Indicator: BPI and Sensitivity Indicator: SI) and resolution chart are used to check the image quality under test condition. The test condition is like as Table I.

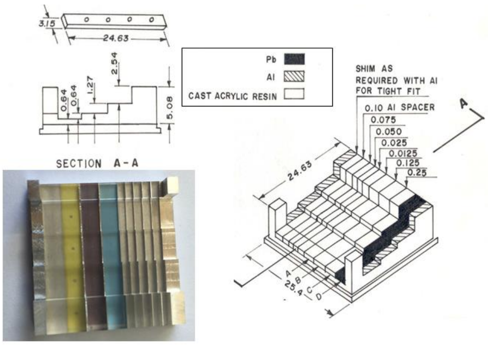

a)

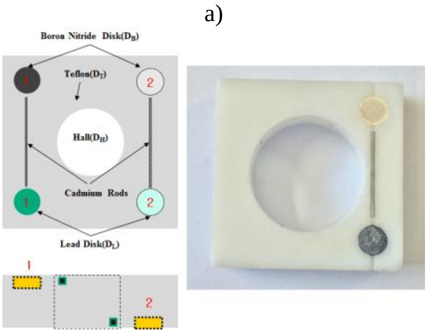

b)

Fig. 3. Schematic Diagram of a) Sensitivity Indicator (SI) and b) Beam Purity Indicator (BPI) [7].

Table I: Test Condition

Parameter	Condition
Exposure time [min]	1, 3, 5
L/D ratio	31, 111
Distance from detector to sample [mm]	0, 50

3. Results and Discussion

Figs.4 and 5 are the neutron images and the contrast profile under exposure time. The L/D ratio is 31 and the standard samples (BPI and SI) was in contact with the detector. As increasing the exposure time from 1 to 5 min, the noise was decreased as shown in Fig.4. Although the L/D ratio is low, the black line (1 mm) of BPI, the black circle (4mm diameter) of BPI and white gap (1 mm) of SI can be easily determined at Fig.4. But, even though the SI has 4 holes with different diameters (0.15, 0.25, and 0.5 mm), it can't be confirmed as shown in Fig.4-b). There are many steps with different thickness and material, each step of SI can be clearly distinguished because of contrast difference on neutron image as shown in Fig.4.

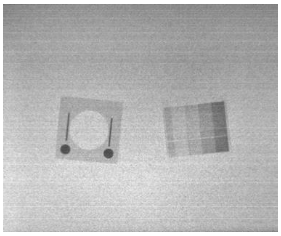

a)

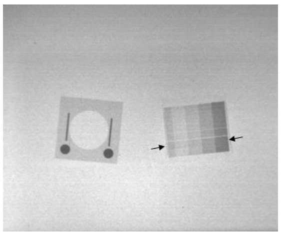

b)

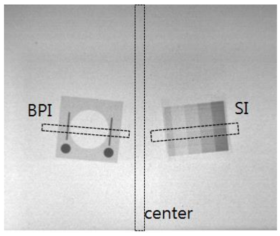

c)

Fig. 4. Neutron Images of SI and BPI with different exposure time: a) 1 min, b) 3 min and c) 5 min.

The neutron beam isn't uniform based on Fig.5(a). The contrast is the highest at the bottom of the image and their deviation is about 22 and 30 % based on Fig.5(a), respectively. Although the contrast value of BPI and SI agrees with the material and thickness as shown in Fig.5(b), the contrast value is not proportional to the thickness. These variations should be considered because they affect the quantitative analysis.

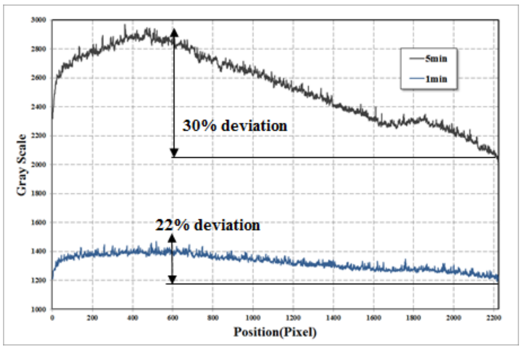

a)

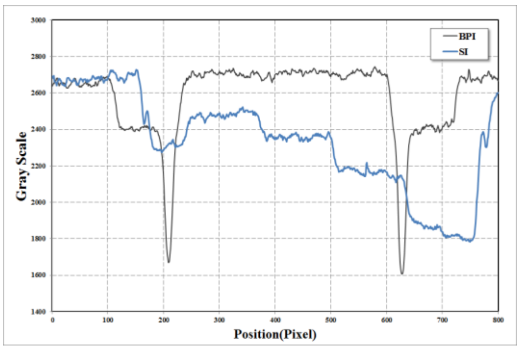

b)

Fig. 5. Contrast Profile at 5 min exposure time: a) center, b) BPI and SI.

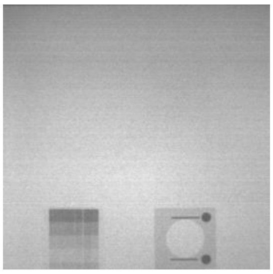

Fig. 6. Neutron image at 50 mm distance from detector to standard specimen(SI and BPI) with 5 min exposure time.

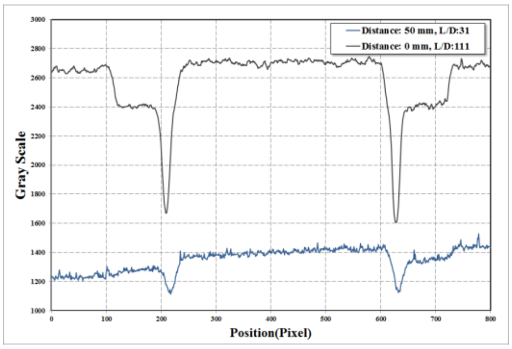

a)

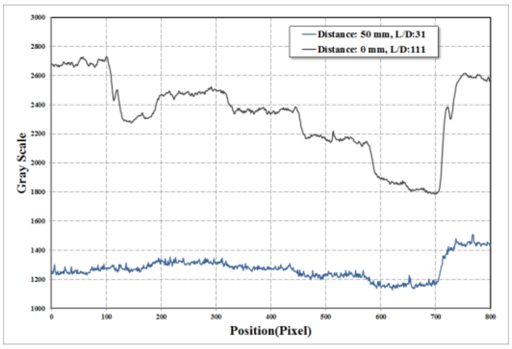

b)

Fig. 7. Contrast Profile comparison with different distance at: a) BPI and b) SI.

Figs.6 and 7 are the neutron image and the contrast profile which is taken at different L/D ratio and different distance from the detector to the sample. The black line of BPI, black circle of BPI and white gap of SI can be also determined at Fig.6. However, as the size of beam exit decreased from 159 × 159 mm^2 to 45 × 45 mm^2 in order to increase the L/D ratio, the contrast value also decreased as shown in Fig. 7. The contrast value of BPI agrees with the material, but the change of contrast according to the material is not so great when compared to the case of the highest neutron flux (L/D: 31) as shown in Fig.7(a). Furthermore, the case of SI is more serious. Although five steps can be easily confirmed in the case of highest neutron flux, it is not easy to distinguish each step because of the low contrast and high blurring as shown in Fig.7(b).

We have measured the spatial resolution of a RANS detector system based on ^{6}LiF doped ZnS scintillator screens using the micro-fabricated test device. Fig. 8(a) shows the neutron image of resolution chart. The resolution is derived by cut-off frequency given in line pairs mm^{-1}(lpm). Although the resolution is 2 lpm from contrast value of cut-off frequency, it is not easy to confirm with eyes.

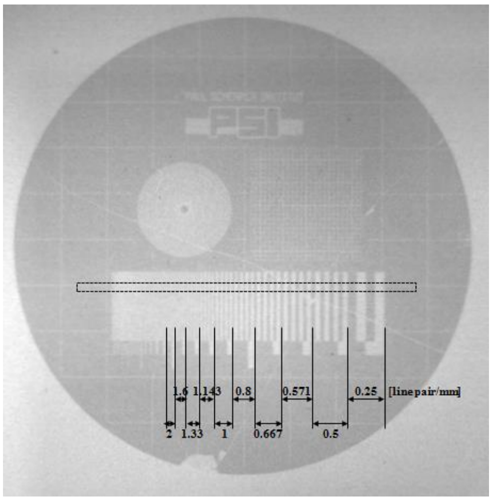

a)

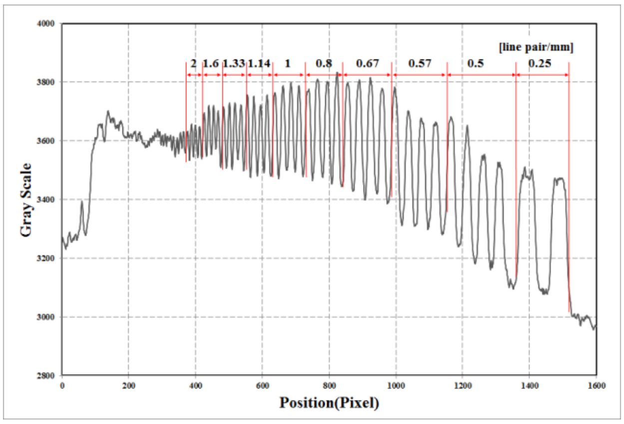

b)

Fig. 8. a) Neutron image of resolution chart and b) contrast profile.

4. Conclusions

We investigated the performance of RANS using the standard samples and resolution chart. Although there is non-uniformity of the neutron beam, RANS has good resolution and contrast with the material and thickness. A compact neutron source is useful, when the observed object has sufficient sensitivity at the available neutron intensity, time resolution, and spatial resolution. It is suggested that the range of applications of compact neutron sources will be increase further because of their flexibility and availability.

ACKNOWLEGMENT

This work was supported by the Korea Atomic Energy Research Institute R&D program and the National Research Foundation of Korea(NRF) grant funded by the Korean government(MSIP:Ministry of Science, ICT and Future Planning) (No. 2012M2A2A6004262)

REFERENCES

[1] Barton, J.P., Multi-purpose neutron radiography system, Proceedings of 5thWorld Conference on Neutron Radiography, 1996.
[2] Filges and F. Goldenbaum, Handbook of Spallation Research, Wiley-VCH (Weinheim, 2009).
[3] A. Taketani, M. Yamada, Y. Ikeda, T. Hashiguchi, H. Sunga, Y. Wakabayashi, S. Ashigai, M. Takamura, S. Mihara, S. Yanagimachi, Y. Otake, T. Wakabayashi, K. Kono and T. Nakayama, Visualization of Water in Corroded Region of Painted Steels at a Compact Neutron Source, ISIJ International, Vol. 57, No. 1, pp. 155–161, 2017
[4] Y. Yamagata, K. Hirota, J. Ju, S. Wang, S. Morita, J. Kato, Y. Otake, A. Taketani, Y. Seki, M. Yamada, H. Ota, U. Bautista and Q. Jia: J. Radioanal. Nucl. Chem., 305, No. 3, 787, 2015
[5] T. Sato, K. Niita, N. Matsuda, S. Hashimoto, Y. Iwamoto, S. Noda, T. Ogawa, H. Iwase, H. Nakashima, T. Fukahori, K. Okumura, T. Kai, S. Chiba, T. Furuta and L. Sihver: J. Nucl. Sci. Technol., 50, 913, 2013.
[6] Y. Ikeda, A. Taketani, M. Takamura, H. Sunaga, M. Kumagai, Y. Oba, Y. Otake and H. Suzuki: Nucl. Instrum. Methods Phys. Res. A, 833, 61, 2016.
[7] ASTM, Standard Test Method for Determination Image Quality in Direct Thermal Neutron Radiographic Examination, West Conshohocken, 2010